Available online at www.sciencedirect.com
ScienceDirect
Inorganic Chemistry Communications 10 (2007) 1355–1359
INORGANIC CHEMISTRY COMMUNICATIONS
www.elsevier.com/locate/inoche

Mixed-ligand platinum and palladium complexes based on dinitrogen chelating ligands and a pyridine bearing the nitronylnitroxide radical

Ahsan M. Shemsi [a,b], Bassam El Ali [a], Khalil A. Ziq [c], Mohamed Morsy [a], Tony D. Keene [d], Silvio Decurtins [d,*], Mohammed Fettouhi [a,*]

[a] Department of Chemistry, King Fahd University of Petroleum and Minerals, Dhahran 31261, Saudi Arabia
[b] PAEC, P.O. Box 1331 Islamabad, Pakistan
[c] Department of Physics, King Fahd University of Petroleum and Minerals, Dhahran 31261, Saudi Arabia
[d] Departement für Chemie und Biochemie, Universität Bern, Freiestrasse 3, CH-3012 Bern, Switzerland

Received 31 July 2007; accepted 16 August 2007
Available online 29 August 2007

Abstract

Novel cationic mixed-ligand palladium and platinum complexes based on the chelating ligands 4,7-dimethyl-1,10-phenanthroline and 2,2′-bipyridine with a pyridine bearing the nitronylnitroxide radical are reported. The synthesis, X-ray crystal structures and magnetic properties of the two complexes [Pd(4,7-dimethyl-1,10-phenanthroline)(NIT-pPy)$_2$](PF$_6$)$_2$. DMF and [Pt(2,2′-bipyridine-*N,N′*)(NIT-pPy)$_2$](PF$_6$)$_2$ · 0.25H$_2$O, (where NIT-pPy = 2-(p-pyridyl)-4,4,5,5-tetramethylimidazoline-1-oxyl-3-oxide) are described. The two metal complexes show a strained square planar geometry. Short intermolecular contacts take place through the nitroxide groups and weak intermolecular antiferromagnetic interactions are dominant at low temperature.

Keywords: Palladium; Platinum; Nitronylnitroxide; X-ray crystal structures; Magnetic properties

The field of molecular magnetic materials has become a rapidly growing area due to the rich variety of physical phenomena with potential applications in future molecular devices [1–4]. Among the various synthetic strategies, coordination chemistry of nitronylnitroxide radical based ligands afforded, in addition to 1D [5–7] and 2D systems [8,9], a large number of discrete molecular species [10–12]. In this context, the coordination chemistry of palladium(II) and platinum(II) metal ions with ligands bearing nitronylnitroxide radicals remains relatively poorly explored [13–19], whereas mixed-ligand complexes based on dinitrogen chelating ligands and pyridylnitronylnitroxide radicals are unknown in the literature. This chemistry possesses relevant aspects. On one hand the potential synergy between the anticipated optical properties of the complexes and their magnetic properties may lead to unusual phenomena [20]. On the other hand the structural planarity of the complexes may assist in the control of the molecular packing. This perspective is supported by the discovery on many occasions of intramolecular exchange interactions through a diamagnetic transition metal spacer [17] [and references therein]. We have previously reported a variety of discrete molecular systems [11]. We have also given evidence to unusual metal-dependent magnetism in square planar Pd/Pt complexes based on nitronylnitroxide bearing ligands [21]. In continuation of this endeavor, we report herein the first examples of mixed-ligand platinum and palladium complexes based on chelating ligands of the type of phenanthroline and bipyridine derivatives with pyridines

* Corresponding authors. Fax: +966 3 860 42 77 (M.Fettouhi); fax: +41 31 631 39 95 (S. Decurtins).
E-mail addresses: silvio.decurtins@iac.unibe.ch (S. Decurtins), fettouhi@kfupm.edu.sa (M. Fettouhi).

1387-7003/$ - see front matter © 2007 Elsevier B.V. All rights reserved.
doi:10.1016/j.inoche.2007.08.013

bearing nitronylnitroxide radicals. The synthesis, X-ray crystal structures and magnetic characterization of [Pd(4,7-dimethyl-1,10-phenanthroline)(NIT-pPy)$_2$](PF$_6$)$_2$ · DMF (**1**) and [Pt(2,2′-bipyridine-*N,N′*)(NIT-pPy)$_2$](PF$_6$)$_2$ · 0.25H$_2$O (**2**) are described (see Scheme 1).

The reaction of Pd(4,7-dimethylphenanthroline)(CF$_3$-COO)$_2$ with NIT-pPy in methanol, followed by precipitation of the hexafluorophosphate salt, leads to the formation of compound (**1**) in good yield [22]. While the synthesis of compound (**2**) necessitates a reflux of Pt(2,2′-bipyridine-*N,N′*)Cl$_2$ with NIT-pPy in methanol/water and a subsequent precipitation of the hexafluorophosphate salt [23]. The solution EPR spectra are typical for a nitronylnitroxide moiety [24]. To the best of our knowledge these are the first examples of mixed-ligand palladium and platinum complexes based on chelating dinitrogen ligands with pyridines bearing nitronylnitroxide radicals.

The X-ray structures of (**1**) and (**2**) are depicted in Figs. 1 and 3 respectively [25]. In compound (**1**), the palladium ion is bonded to the phenanthroline ligand and two p-pyridyl radical ligands in a typical strained square planar geometry. Both Pd–N$_{py}$ and Pd–N$_{phen}$ bond distances are in the same range and average to 2.016(5) Å, in agreement with the values reported in similar compounds [28]. The chelating ligand strain imposes an bond angle N1–Pd1–N2 of 81.7(2)°, while the corresponding angle involving the two pyridyl ligands is N3–Pd1–N6 of 87.05(18)°. The first nitronylnitroxide ligand has its pyridyl mean plane almost coplanar (3.8(6)°) with the O(1)N(4)C(20)N(5)O(2) moiety while being essentially orthogonal to the PdN$_4$ mean plane with an angle of 89.7(1)°. The second nitronylnitroxide ligand exhibits significant geometrical differences. Its pyridyl mean plane is tilted with 23.1(6)° from the O(3)N(7)C(32)N(8)O(4) moiety mean plane. It also deviates significantly from orthogonality with the PdN$_4$ plane, the angle being 83.9(2)°. The shortest intermolecular contacts, corresponding to distances less the sum of van der Waals radii [29], take place between the oxygen atoms of the nitroxide groups and the phenanthroline nitrogen atoms of the adjacent molecules (O2···N1: 3.066 Å and O4···N2: 2.984 Å). This interaction scheme gives rise to one dimensional molecular chains developing along the *c* axis (Fig. 2).

The structural features of compound (**2**) are similar to those of compound (**1**). The platinum ion is bonded to the bipyridine ligand and two p-pyridyl nitronyl nitroxide

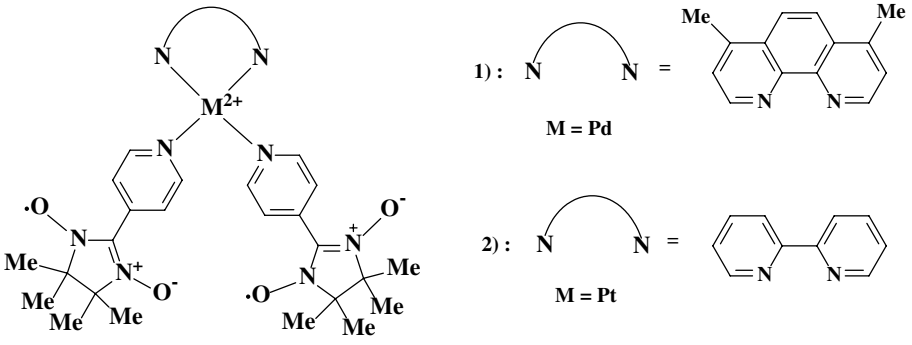

Scheme 1.

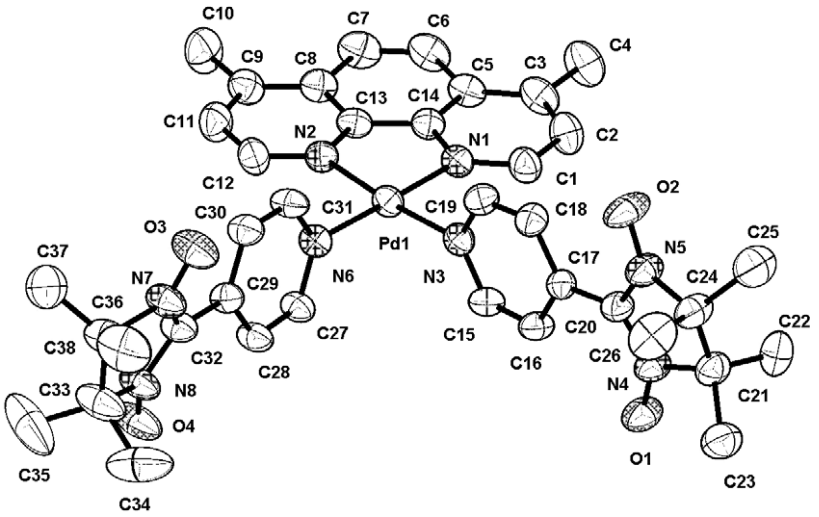

Fig. 1. Molecular structure of (**1**). The thermal ellipsoids are drawn at the 30% probability level. Hydrogen atoms, PF_6^- ions and the solvent molecule are omitted for clarity.

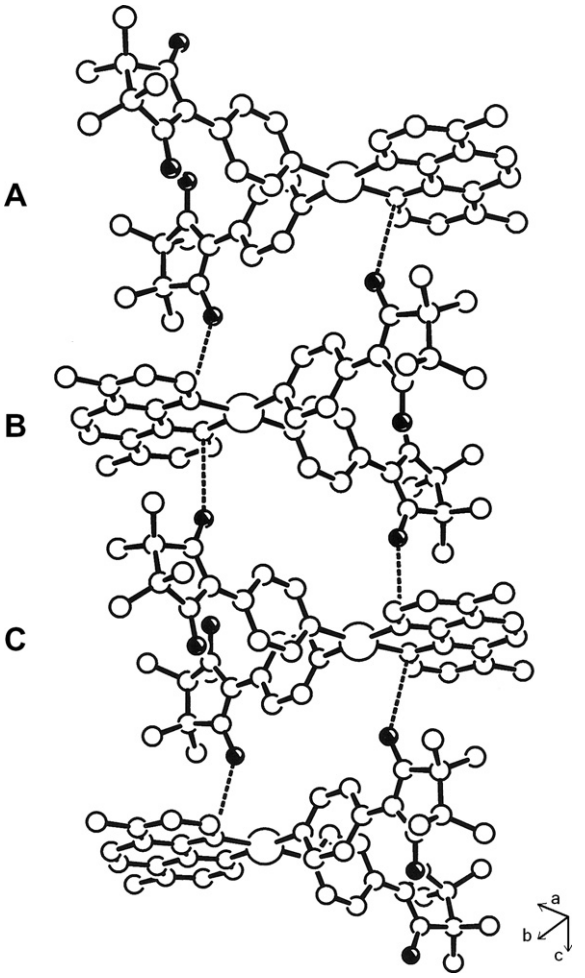

Fig. 2. Structure of the molecular chains in (**1**).

ligands in a strained square planar geometry. The average Pt–N bond distance is 2.014(7) Å, in agreement with the values reported in similar compounds [30,31]. The chelating ligand strain imposes a bond angle N1–Pt1–N2 of 80.7(3)°, while the angle involving the two pyridyl ligands is N6–Pt1–N3 of 87.3(3)°. The pyridyl mean plane of one nitronylnitroxide ligand deviates from coplanarity with the O(4)N(8)C(28)N(7)O(3) moiety with an angle of 4.9(4)°. It also makes an angle of 86.3(3)° with the PtN_4 mean plane, whereas, for the second nitronylnitroxide ligand, the pyridyl mean plane is tilted 11.5(9)° from the O(1)N(4)C(16)N(5)O(2) moiety mean plane and the angle with the PtN_4 mean plane is 87.4(2)°. In this case also, the shortest intermolecular contacts take place between the oxygen atoms of the nitroxide groups and the bipyridine nitrogen atoms of the adjacent molecules (O1···N1: 2.912 Å and O4···N2: 3.093 Å). This interaction scheme is also consistent with one dimensional molecular chains developing along the [110] direction.

The molar magnetic susceptibility of compound (**1**) [33] shows a Curie–Weiss behavior above 40 K (Fig. 4). The data were corrected for partial radical decomposition in the sample [34] and a fit to the $S = 1/2$ antiferromagnetic dimer model was found appropriate with an interaction occurring between the nitronylnitroxide radicals, giving $C = 0.3859(2)$ cm^3 K mol^{-1} and $\theta = -0.36(8)$ K. The room

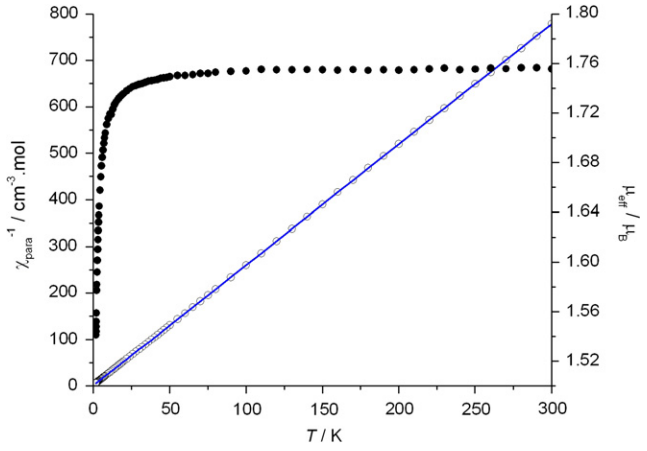

Fig. 4. Corrected inverse molar susceptibility, χ^{-1}(T) of (**1**) (open circles) with Curie–Weiss fit (line) and of μ_{eff}(T) (closed circles).

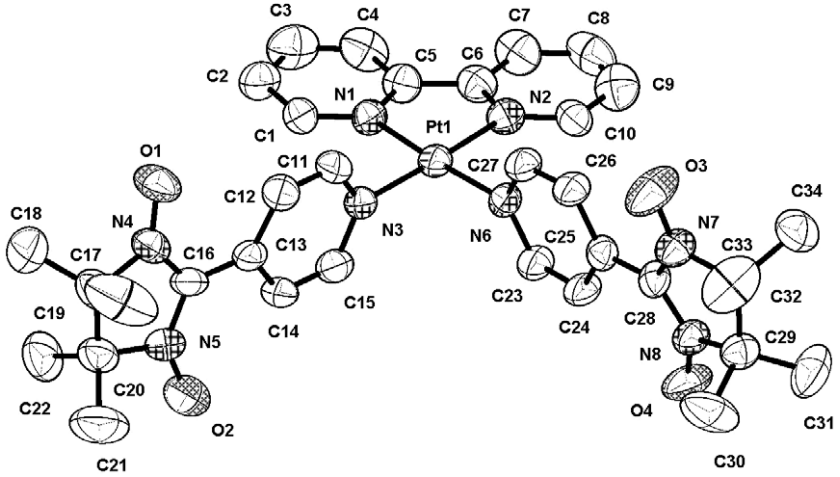

Fig. 3. Molecular structure of (**2**). The thermal ellipsoids are drawn at the 30% probability level. Hydrogen atoms, the water molecule and the PF_6^- ions are omitted for clarity.

temperature magnetic moment of 1.75 μ_B is in good agreement with the spin-only prediction of 1.73 μ_B. There are two possible magnetic dimeric units in compound (**1**). A first intramolecular dimer in which the two radical ligands interact through a 14 bonds pathway within the complex. This pathway is very long and unlikely to be effective. A second magnetic dimer, intermolecular in nature, involves a radical from molecule A interacting with a radical from a molecule C through short O···N contacts of the nitronyl groups of the two radicals with a phenanthroline ligand belonging to an intermediate molecule B (Fig. 2). The latter dimer occurs via two O···N short contacts together with two possible bond pathways. The first scheme [O···N–C–C–N···O] involves the phenanthroline molecular orbital only, where the oxygen orbital overlaps with the HOMO π-orbital of the phenanthroline. The two radicals are then interacting antiferromagnetically through the same molecular orbital. The second [O···N–Pd–N···O] scheme includes the metal-phenanthroline half coordination sphere where the oxygen orbital overlaps with the phenanthroline LUMO π*-orbital interacting with the d-orbitals of the metal ion. The latter orbitals, being orthogonal to each other, yield a ferromagnetic interaction. The overall coupling strength is a combination of the two interactions.

The molar magnetic susceptibility of compound (**2**) shows also a Curie–Weiss behavior above 100 K (Fig. 5). Similarly to compound (**1**), the data were corrected for partial radical decomposition in the sample [35] and a fit to the $S = 1/2$ antiferromagnetic dimer model was found appropriate with an interaction occurring between the nitronylnitroxide radicals, giving $C = 0.3681(2)$ cm^3 K mol^{-1} and $\theta = -0.02(12)$ K. The room temperature magnetic moment was found 1.72 μ_B, in good agreement with the spin-only predicted value of 1.73 μ_B. As with compound (**1**), the same dimeric interaction between two molecules through a third one is likely to be responsible for the coupling. The compounds show similar couplings, in the region of a few tenths of a Kelvin, and similar amounts of partial radical decomposition, which is accounted for by the modified dimer equation. The small difference in the coupling is likely to be due to differences in the pathway effectiveness within the 'bridging' molecule π-orbitals and through the π*-d orbitals. It can be speculated that the coupling in compound (**2**) is smaller for two reasons. The character of the C–C bridge in 2,2′-bipyridine is more σ-like [36], hence reducing the overlap of π-orbitals between the two pyridine rings and possibly the strength of the coupling across them in comparison to the phenanthroline molecule. At the same time, the overlap of the d-orbitals with the LUMO is likely to be better due to the larger and more diffuse nature of the 5d orbitals in Platinum compared with the 4d orbitals of Palladium, so giving a larger ferromagnetic contribution. The combined effects of the reduced antiferromagnetic contribution and the increased ferromagnetic contribution could give a smaller antiferromagnetic net coupling in compound (**2**). While the proposed relationship fits well with the data and values obtained from the models, some caution must be taken as the interaction strength is small compared to the lowest recorded temperature in the measurements.

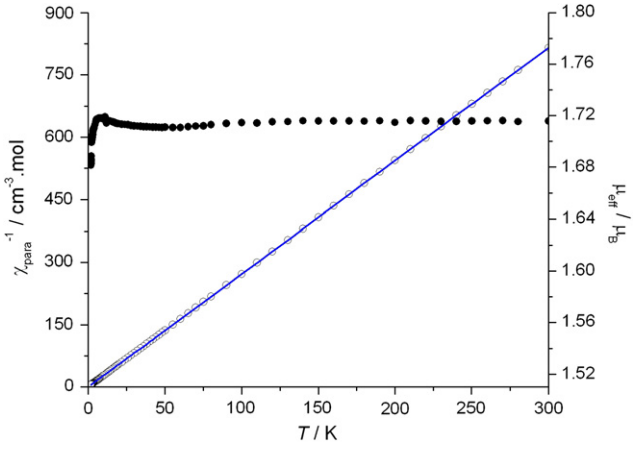

Fig. 5. Corrected inverse molar susceptibility, χ^{-1}(T) of (**2**) (open circles) with Curie–Weiss fit (line) and of μ_{eff}(T) (closed circles).

Acknowledgement

We gratefully acknowledge King Fahd University of Petroleum and Minerals – Dhahran – Saudi Arabia for the financial support under KFUPM research project CY/METAL/301.

Appendix A. Supplementary material

CCDC 623,335 and 623,334 contain the supplementary crystallographic data for **1** and **2**. These data can be obtained free of charge via http://www.ccdc.cam.ac.uk/conts/retrieving.html, or from the Cambridge Crystallographic Data Centre, 12 Union Road, Cambridge CB2 1EZ, UK; fax: (+44) 1223-336-033; or e-mail: deposit@ccdc.cam.ac.uk. Supplementary data associated with this article can be found, in the online version, at doi:10.1016/j.inoche.2007.08.013.

References

[1] K. Itoh, M. Kinoshita (Eds.), Mol. Magn., Gordon and Breach, Amsterdam, 2000.
[2] O. Kahn, Mol. Magn., VCH, New York, 1993.
[3] J.S. Miller, A.J. Epstein, W.M. Reiff, Chem. Rev. 88 (1988) 201.
[4] D. Luneau, P. Rey, Coord. Chem. Rev. 249 (2005) 2591.
[5] K. Bernot, L. Bogani, A. Caneschi, D. Gatteschi, R. Sessoli, J. Am. Chem. Soc. 128 (2006) 7947.
[6] C. Rajadurai, K. Falk, S. Ostrovsky, V. Enkelmann, W. Haase, M. Baumgarten, Inorg. Chim. Acta. 358 (2005) 3391.
[7] D.-Z. Gao, J. Chen, S.-P. Wang, Y. Song, D.-Z. Liao, Z.-H. Jiang, S.-P. Yan, Inorg. Chem. Commun. 9 (2006) 132.
[8] E. Tretyakov, S. Fokin, G. Romanenko, V. Ikorskii, S. Vasilevsky, V. Ovcharenko, Inorg. Chem. 45 (2006) 3671.
[9] I. Dasna, S. Golhen, L. Ouahab, O. Pena, N. Daro, J-P. Sutter, Cr. Acad. Sci. IIc chem. 4 (2001) 125.
[10] G. Francese, F.M. Romero, A. Neels, H. Stoeckli-Evans, S. Decurtins, Inorg. Chem. 39 (2000) 2087.

[11] M. Fettouhi, B. El Ali, A.M. El-Ghanam, S. Golhen, L. Ouahab, N. Daro, J.P. Sutter, Inorg. Chem. 41 (2002) 3705.
[12] L.-Y. Wang, C.-X. Zhang, D.-Z. Liao, Z.-H. Jiang, S.-P. Yan, J. Coord. Chem. 58 (2005) 969.
[13] M. Ueda, M. Itou, K. Okazawa, T. Mochida, H. Mori, Polyhedron 24 (2005) 2189.
[14] D.B. Leznoff, C. Rancurel, J-P. Sutter, S.J. Rettig, M. Pink, O. Kahn, Organometallics 18 (1999) 5097.
[15] H. Oshio, A. Ohto, T. Ito, Chem. Commun. 13 (1996) 1541.
[16] K.E. Schwarzhans, A. Stuefer, Monatsh. Chem. 114 (1983) 137.
[17] C. Stroh, M. Mayor, C. Von Haenisch, P. Turek, Chem. Commun. 18 (2004) 2050.
[18] M. Ueda, T. Mochida, M. Itou, N. Asanagi, H. Mori, Inorg. Chim. Acta. 348 (2003) 123.
[19] J.R. Gardinier, R. Clerac, F.P. Gabbai, J. Chem. Soc. Dalton Trans. 23 (2001) 3453.
[20] M. Hissler, J.E. McGarrah, W.B. Connick, D.K. Geiger, S.D. Cummings, R. Eisenberg, Coord. Chem. Rev. 208 (2000) 115.
[21] M. Fettouhi, B. El Ali, M. Morsy, S. Golhen, L. Ouahab, B. Le Guennic, J.-Y. Saillard, N. Daro, J.-P. Sutter, E. Amouyal, Inorg. Chem. 42 (2003) 1316.
[22] *Synthesis of compound* (**1**): 0.500 mmol (0.271 g) of Pd(4,7-dimethylphenanthroline)$(CF_3COO)_2$ were dissolved in 50 ml of methanol in a 100 ml erlenmeyer flask. Separately, 1.10 mmol (0.259 g) of NIT-pPy were dissolved in 10 ml of methanol. Both solutions wee mixed and stirred for 4 h at room temperature. The solution was filtered off and NH_4PF_6 1.50 mmol (0.245 g) in 3 ml of methanol was added slowly to the filtrate. A greenish yellow precipitate formed immediately. After 1 h the mixture was filtered and the precipitate washed with cold methanol, vacuum dried and recrystallized from a DMF/methanol (1:10) affording green parallelepipedic crystals (yield: 87%). Anal. Calc for $C_{41}H_{51}N_9O_5P_2$ F_{12}Pd: C, 42.9; H, 4.4; N, 10.99. Found C, 42.4; H, 4.1; N, 10.6%. IR (KBr): 3446, 3114, 2991, 1673, 1615, 1526, 1410, 1374(ν_{NO}), 1317, 1168, 844, 558, 373 cm^{-1}. UV–vis (DMF) λ, nm (ε, $M^{-1}\,cm^{-1}$) 279 (41,300), 367 (19,400).
[23] *Synthesis of compound* (**2**): 0.592 mmol (0.250 g) of Pt(2,2′-bipyridine-*N,N′*)Cl_2 were dissolved in 200 ml of methanol/water (1:1) in a 500 ml erlenmeyer flask. 1.24 mmol (0.292 g) of NIT-pPy were added and the mixture was refluxed at 80 °C for 24 h. The cold solution was filtered off and concentrated in vacuum till 50 ml. 1.24 mmol of NH_4PF_6 (0.203 g) were dissolved in minimum water and added slowly to the filtrate. A brown precipitate formed immediately. It was then filtered, washed with cold methanol, vacuum dried and recrystallized from DMF/acetone (1:10), affording green parallelepipedic crystals (yield: 53%). Anal. Calc. for $C_{34}H_{40.5}N_8O_{4.25}P_2F_{12}$Pt: C, 36.64; H, 3.66; N, 10.05. Found C, 36.55; H, 3.72; N, 10.04%. IR (KBr) 3432, 1668, 1617, 1545, 1455, 1414, 1375(ν_{NO}), 1318, 1168, 839, 770, 558, 373 and 359 cm^{-1}. UV–vis (DMF) λ, nm (ε, $M^{-1}\,cm^{-1}$) 308 (38,900), 320 (41,100), 369 (12,900) and 377 (16,700).
[24] EPR spectra: The solution X-band EPR spectra recorded in dimethylformamide show the typical 5 line pattern (1:2:3:2:1) expected for the coupling with two identical nitrogen nuclei ($I = 1$). The hyperfine coupling constants are $a_N \approx 7.2$ G and $a_N \approx 6.7$ G for (**1**) and (**2**) respectively.
[25] X-ray intensity data were recorded on a Bruker-Axs Smart Apex system equipped with a graphite monochromatized Mo Kα radiation ($\lambda = 0.71073$ Å). The data were corrected for Lorentz-polarization and absorption effects. The structures were solved with direct methods and refined by full matrix least square methods based on F^2, using the structure determination and graphics package SHELXTL (version 5.10) [26]. Some graphics were generated using WinGX (version 1.64.05) [27]. Hydrogen atoms were included at calculated positions using a riding model. For (**1**) $C_{41}H_{51}F_{12}N_9O_5P_2$Pd, Mr = 1146.25, green parallelepiped, 0.34 × 0.19 × 0.18 mm, $T = 296$ K, monoclinic, space group $P2_1/n$, $a = 13.7256(14)$ Å, $b = 23.843(3)$ Å, $c = 16.4297(17)$ Å, $\beta = 109.341(2)°$, $V = 5073.4(9)$ $Å^3$, $Z = 4$, $Dc = 1.501$ g cm^{-1}, $\mu = 0.524$ mm^{-1}, $F(000) = 2336$, ω scan mode, θ range = 1.57–28.29°, 44,654 reflections collected, $R_1 = 0.0698$, $wR_2 = 0.1513$ and goodness of fit = 0.947 for 643 refined parameters using 4,867 unique reflections ($R_{int} = 0.1143$) with $I > 2\sigma(I)$. For (**2**) $C_{34}H_{40.5}F_{12}N_8O_{4.25}$ P_2Pt, Mr = 1114.27, green parallelepiped, 0.36 × 0.21 × 0.14 mm, $T = 296$ K, monoclinic, space group C2/c, $a = 22.5767(18)$ Å, $b = 25.556(2)$ Å, $c = 17.6112(14)$ Å, $\beta = 119.368(1)°$, $V = 8855.3(12)$ $Å^3$, $Z = 8$, $Dc = 1.672$ g cm^{-1}, $\mu = 3.338$ mm^{-1}, $F(000) = 4404$, ω scan mode, θ range = 1.31–28.30 °, 39,062 reflections collected, $R_1 = 0.0595$, $wR_2 = 0.1576$ and goodness of fit = 0.987 for 566 refined parameters using 5286 unique reflections ($R_{int} = 0.0639$) with$I > 2\sigma(I)$.
[26] G.M. Sheldrick, SHELXTL V5.1 Software, Bruker AXS, Inc., Madison, Wisconsin, USA, 1997.
[27] L.J. Farrugia, J. Appl. Cryst. 32 (1999) 837.
[28] B. Milani, A. Scarel, E. Zangrando, G. Mestroni, C. Carfagna, B. Binotti, Inorg. Chim. Acta. 350 (2003) 592.
[29] A. Bondi, J. Phys. Chem. 68 (1964) 441.
[30] T. Koshiyama, M. Kato, Acta. Cryst. C 59 (2003) m446.
[31] G.B. Deacon, B.M. Gatehouse, S.T. Haubrich, J. Ireland, E.T. Lawrenz, Polyhedron 17 (1998) 791.
[32] R.L. Carlin, Magnetochemistry, Springer-Verlag, Berlin, 1986.
[33] The magnetic susceptibility and magnetization experiments were carried out between 300 and 1.8 K on a Quantum Designs MPMS XL SQUID magnetometer. Corrections for the diamagnetic components of the samples were initially calculated using literature values of Pascal's constants [2] and refined further by adjusting iteratively the components to produce a horizontal plot in the high-temperature region ($150 < T < 300$ K) of the $\chi T(T)$ plot.
[34] *Magnetic properties of compound* (**1**): The molar paramagnetic susceptibility [33] increases upon cooling to a value of 0.1286(1) $cm^3 \cdot mol^{-1}$ at 1.86 K. An inverse susceptibility plot shows that Curie–Weiss behavior is followed above 40 K and a fit to the data gave $C = 0.3122(1)$ $cm^3 \cdot K \cdot mol^{-1}$ and $\theta = -0.36(8)$ K. The Curie constant is low compared to the predicted value of 0.375 for an $S = 1/2$ system and so is the derived *g*-value (1.824) which is likely due to partial radical decomposition of the sample. The spins on the radicals can be taken as isotropic and the Heisenberg Hamiltonian ($H = -2J_{ij}\,\boldsymbol{S}_i \cdot \boldsymbol{S}_j$) applies [32]. Given the molecular composition of (**1**) and the negative Weiss constant, a fit to the $S = 1/2$ antiferromagnetic dimer model is appropriate with an interaction occurring between the nitronlynitroxide radicals. To account for the partial radical decomposition of the sample, a model of the molar paramagnetic susceptibility for $S = 1/2$ dimers [32] modified with a scale factor, *p*, was used.

$$\chi_{para} = p \cdot \frac{Ng^2\mu_B^2}{3k_BT} \cdot [1 + 1/3\exp(-2J/k_BT)]^{-1}$$

The *g*-value was fixed to 2.0, giving $J = -0.68(1)$ K and $p = 80.7(2)$%, indicating that 19.3% of the sample had decomposed. After adjusting the data accordingly, a Curie–Weiss fit (Fig. 4) gave $C = 0.3859(2)$ cm^3 K mol^{-1} and $\theta = -0.36(8)$ K. A plot of the effective moment (Fig. 4) gives a room temperature moment of 1.75 μ_B which is in good agreement with the spin-only prediction of 1.73 μ_B.
[35] *Magnetic properties of compound* (**2**): The molar paramagnetic susceptibility increases upon cooling to a value of 0.1545 $cm^3 \cdot mol^{-1}$ at 1.87 K. An inverse susceptibility plot showed that Curie–Weiss behavior is followed above 100 K. In this case also the Curie constant is low at 0.3005(2) cm^3 K mol^{-1} with $\theta = -0.13(7)$ K. The susceptibility was modeled by the same equation as compound (**1**) with *g* fixed at 2.0. The resulting values are $J = -0.20(1)$ K and $p = 81.6(1)$%. The susceptibility data were corrected by this factor and an inverse susceptibility plot (Fig. 5) gave $C = 0.3681(2)$ $cm^3 \cdot K \cdot mol^{-1}$ and $\theta = -0.02(12)$ K. A plot of the effective moment (Fig. 5) gives a room temperature moment of 1.72 μ_B, which shows a good agreement with the spin-only value.
[36] H.W. Park, S.M. Sung, K.S. Min, H. Bang, M.P. Suh, Eur. J. Inorg. Chem. (2001) 2857.